

# Determinants of Directionality and Efficiency of the ATP Synthase $F_o$ Motor at Atomic Resolution

Antoni Marciniak, Pawel Chodnicki, Kazi A Hossain, Joanna Slabonska, and Jacek Czub\*



Cite This: *J. Phys. Chem. Lett.* 2022, 13, 387–392



Read Online

ACCESS |



Metrics & More

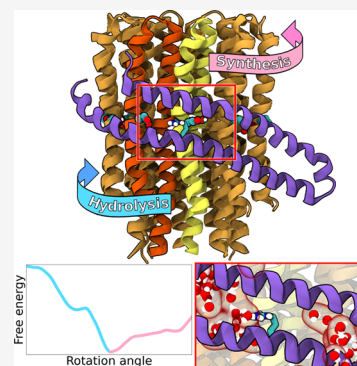


Article Recommendations



Supporting Information

**ABSTRACT:**  $F_o$  subcomplex of ATP synthase is a membrane-embedded rotary motor that converts proton motive force into mechanical energy. Despite a rapid increase in the number of high-resolution structures, the mechanism of tight coupling between proton transport and motion of the rotary c-ring remains elusive. Here, using extensive all-atom free energy simulations, we show how the motor's directionality naturally arises from the interplay between intraprotein interactions and energetics of protonation of the c-ring. Notably, our calculations reveal that the strictly conserved arginine in the a-subunit (R176) serves as a jack-of-all-trades: it dictates the direction of rotation, controls the protonation state of the proton-release site, and separates the two proton-access half-channels. Therefore, arginine is necessary to avoid slippage between the proton flux and the mechanical output and guarantees highly efficient energy conversion. We also provide mechanistic explanations for the reported defective mutations of R176, reconciling the structural information on the  $F_o$  motor with previous functional and single-molecule data.



$F_oF_1$ -ATP synthase is a ubiquitous multisubunit protein that reversibly couples the proton gradient across energy-transducing membranes to the synthesis of ATP from ADP and inorganic phosphate.<sup>1</sup> It consists of two mechanically coupled rotary motors: the hydrophilic  $F_1$ , driven by ATP hydrolysis, and the membrane-embedded  $F_o$ , powered by proton translocation across the membrane.<sup>2–5</sup> Two components of  $F_o$  that are directly involved in this transport are the c-ring, i.e., a rotating oligomer of c-subunits, and the stator a-subunit that wraps around the c-ring (Figure 1) to form two hydrated proton-access half-channels.<sup>4,6–10</sup>

During mitochondrial ATP synthesis, protons from the perimitochondrial space bind to the conserved carboxylate near the middle of the c-subunit at proton-binding half-channel (B, yellow in Figure 1) and are released to the matrix when the same c-subunit reaches the release half-channel (R; red) after almost 360° rotation (magenta pathway).<sup>9,11–16</sup> As a result, proton flow through  $F_o$  induces counterclockwise (when viewed from the matrix) rotation of the c-ring relative to the a-subunit, generating torque that drives the rotation of  $F_1$ , and eventually leads to ATP synthesis.<sup>17,18</sup>

The question that arises is how  $F_o$  ensures unidirectional rotation of the c-ring preventing futile proton leakage, a necessary condition for a remarkably high efficiency of the free energy transduction.<sup>19,20</sup> Because the rotation by one c-subunit in either direction leads to equivalent states, the synthesis direction has to be kinetically preferred; i.e., the energetic barrier along the mechanical coordinate should be markedly lower in the synthesis direction than in the hydrolysis direction.

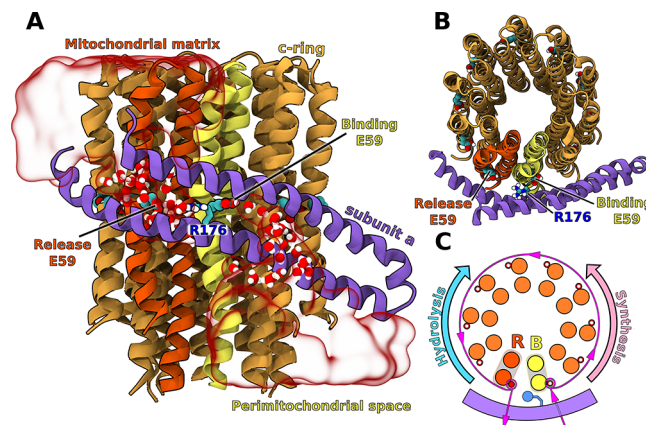
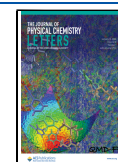


**Figure 1.** Side (A) and top (B) view of the c-ring/a-subunit interface. Transparent red surface shows representative water distribution in the two half-channels (for average water density, see Figure S1). The c-subunits shown in yellow and red mark the binding (B) and release (R) sites for protons in the synthesis mode. Only residues 152–249 in the a-subunit are shown for clarity. For full subunit composition of the simulated  $F_o$ , see Figure S2. (C) Proton transfer pathway through  $F_o$  in the synthesis mode. In the ATP hydrolysis-driven pumping mode, the c-ring rotates in the reverse direction.

Received: October 12, 2021

Accepted: January 3, 2022

Published: January 5, 2022



This kinetic preference has been proposed to arise from the specific interactions between the central arginine residue in the a-subunit (R176 in Figure 1) and carboxylates in the proton binding and release half-channels.<sup>21,22</sup> Indeed, mutational studies have shown that the central arginine is essential for coupling proton translocation to mechanical motion and preventing proton leakage.<sup>23–25</sup> Because the Arg residue is located right in the middle between the R and B half-channels (Figure 1B), its electrostatic attraction to the freshly deprotonated carboxylate at site R should favor the rotation in the synthesis direction and oppose the reverse rotation.<sup>26–28</sup> By determining the free energy landscapes using a coarse-grained model, Bai and Warshel have recently shown that this simple electrostatic view of the  $F_o$  directionality only holds if the energetics of proton transfer to the carboxylates is included, ensuring the asymmetric attraction between Arg and the R and B sites.<sup>13,29,30</sup>

While these findings explain the general aspects of the mechanochemical coupling, they do not provide atomic-level understanding of the  $F_o$  mechanism; in particular, it is not known why Arg is strictly conserved and cannot be substituted by a positively charged Lys residue that could act in an analogous manner. Here, by using atomistic molecular dynamics-based free energy simulations (total sampling time of nearly 70  $\mu$ s), we provide a detailed insight into the origin of the directionality of the c-ring rotation and elucidate the role of the central arginine in the  $F_o$  mechanism.

To understand the mechanism of action of  $F_o$  in atomic detail, we determined and compared the free energy profiles for the rotation of the yeast mitochondrial  $F_o$  by one c-subunit in the synthesis and hydrolysis directions (+36° and -36°, respectively, in Figure 2; for details see Supporting

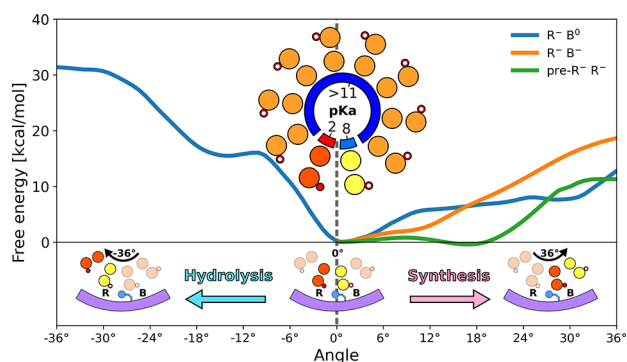


**Figure 2.** Free energy profiles for the  $F_o$  rotation in hydrolysis and synthesis direction by one c-subunit ( $0^\circ \rightarrow 36^\circ$ ), at different protonation states of the c-ring. Inset in the middle shows the computed  $pK_a$ 's of the c-ring carboxylates (at  $0^\circ$  position, as captured by the cryo-EM structure).<sup>5</sup> For convergence of the free energy profiles, see Figures S4–S6.

Information, Methods). Because energetics of the c-ring rotation has been found to strongly depend on the protonation state of the B and R carboxylates,<sup>30</sup> we first calculated their  $pK_a$ 's in the  $F_o$  initial state ( $0^\circ$ ) using the alchemical approach (Supporting Information, Methods). We found (inset in Figure 2) that  $pK_a$  of the B site ( $8.4 \pm 0.3$ ) is markedly higher and that of the R site ( $1.9 \pm 0.2$ ) is markedly lower compared to pH of their respective compartments (e.g., 6 and 7, respectively), even if the predicted shifts are somewhat overestimated. This finding suggests that proton affinities for

the B and R sites are fine-tuned to the proton gradient direction, promoting the rate of the proton transfer via  $F_o$  under physiological conditions. The observed difference in  $pK_a$  between the B and R sites seems to result mostly from a different degree of hydration of both carboxylates (see also discussion below and Supporting Information for further details). The  $pK_a$  values for the remaining eight proton-carrying c-subunits that are exposed mostly to lipid environment (see Figure S3) were computed to be at least 11.

As can be seen, the free energy profiles determined for the dominant protonation state (deprotonated R, protonated B,  $R^-B^0$ ; blue curves in Figure 2) are locally strongly asymmetric around  $0^\circ$ , implying a  $\sim 15$  kcal/mol kinetic preference for the rotation in the synthesis direction, consistent with the previous models of the motor's unidirectional motion.<sup>13,21,26,27,30</sup>

It has been suggested, however, that not only protonation thermodynamics (as described by  $pK_a$ 's) but also the rate of (de)protonation might play an important role in the directional rotary mechanism.<sup>30</sup> In particular, protonation of the B site could even be expected to be a rate limiting step, given that a single file of water molecules confined between the helices of the a-subunit connects this site to the rest of the half-channel (as seen in Figure 1 and Figure S1, consistent with previous cryo-EM data).<sup>7,31,32</sup> Therefore, we examined the effect of the B site deprotonation on the rotation energetics by recomputing the free energy of the rotation in the synthesis direction with both R and B sites deprotonated ( $R^-B^-$ ; orange curve in Figure 2).

As can be seen, beyond  $10^\circ$  the  $R^-B^-$  profile rapidly increases with a roughly constant slope of 1.8 kcal/(mol·deg), reflecting the change of environment around the B site carboxylate from polar and partially hydrated (at  $0^\circ$ ) to fully hydrophobic (at  $36^\circ$ ). This increase effectively inhibits the full rotary step in this protonation state ensuring that the c-ring waits, if necessary, for the protonation of the B site to occur. Surprisingly, however, in the range up to  $10^\circ$ , the  $R^-B^-$  protonation state seems to kinetically favor the synthesis direction even more than the  $R^-B^0$  protonation state, as the free energy barrier for the former is  $\sim 3$  kcal/mol lower. Since the two curves change their slope around  $10^\circ$ , with  $R^-B^-$  becoming notably steeper and  $R^-B^0$  flatter, it may suggest that the c-ring, starting from  $0^\circ$ , first tends to rotate with the B site carboxylate deprotonated up to  $10^\circ$ , where it stalls waiting for the carboxylate to get protonated, to progress further governed by the less steep  $R^-B^0$  profile. This hypothesis would agree with previous structural studies and the recent single-molecule study that revealed the existence of a  $11^\circ$  substep in the rotary mechanism of the *E. coli*  $F_o$ .<sup>33,34</sup> To test whether at  $10^\circ$  the B carboxylate is still connected to water in the proton-binding half-channel, we calculated the carboxylate–water radial distribution function (Figure S7) and found that upon  $10^\circ$  rotation the degree of hydration increases substantially, possibly making the proton binding from the half-channel even more efficient than at  $0^\circ$ . Increasing hydration of the B carboxylate may also account for an unexpectedly flat rotation free energy in the  $R^-B^-$  protonation state in the  $0$ – $10^\circ$  range. Consistently, a doubly deprotonated state of the c-ring was also found to contribute to the proton transfer pathway in the recent coarse-grained simulations.<sup>13</sup>

Because during the rotation in the synthesis direction the c-subunit entering the R site (pre-R subunit) moves from hydrophobic to polar and well-hydrated environment (Figures S1, S3, S7, and S8), which corresponds to a drastic decrease in

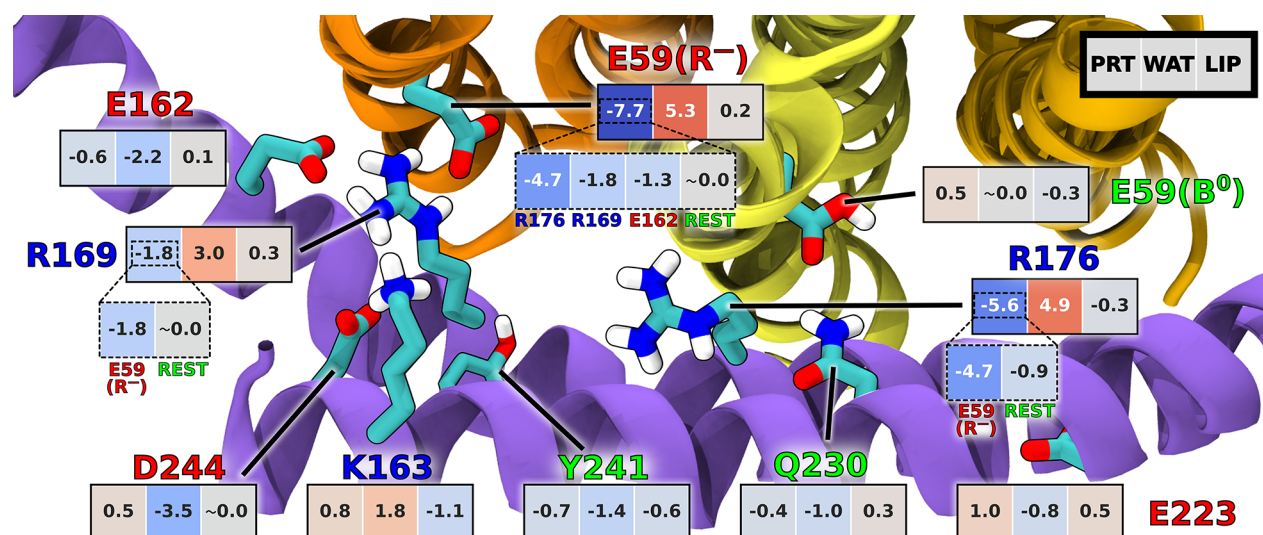


**Figure 3.** Comparison of the per-residue enthalpic contributions to the rotation free energies in the synthesis and hydrolysis direction. Values shown are the differences in the average slopes of these contributions with respect to the rotation angle between the synthesis and hydrolysis directions, calculated in the 0–18° range. Accordingly, negative values indicate the contributions favoring the rotation in the synthesis direction and vice versa. Interactions of each residue within the protein (PRT) and with water (WAT) and lipids (LIP) are shown separately. Only residues with any of the slope differences exceeding 1.0 kcal/(mol-deg) are included (with exception of E59(B<sup>0</sup>); see Figures S9–S12 for complete pairwise data).

the  $pK_a$  of E59, early deprotonation of the pre-R carboxylate can also be expected to affect the rotation kinetics. To test this possibility, we determined the effect of deprotonation of the pre-R carboxylate on the synthesis free energy profile [(pre-R)<sup>-</sup>R<sup>-</sup>; green curve in Figure 2]. We found that for the (pre-R)<sup>-</sup>R<sup>-</sup> state, as opposed to the two other examined protonation states, the profile remains virtually flat up to 20°, which shows that early proton release might in fact promote faster progression of the c-ring in the synthesis direction, further highlighting the coupling between rotation and (de)protonation events.

Next, to gain atomic-level understanding of the directionality mechanism, we examined residue–residue and residue–environment enthalpic contributions to the interaction free energies along the mechanical coordinate (see Supporting Information Methods for details). In Figure 3, the average local slopes of the corresponding contributions in the synthesis and hydrolysis direction were subtracted from each other such that the resulting negative values indicate the interactions favoring the c-ring rotation in the synthesis direction over the hydrolysis direction and vice versa. It can be clearly seen that the attractive interaction between the deprotonated E59 at the release site (R<sup>-</sup>) and the central R176, stably oriented towards the R site (see also Figure S13), is a key differentiating factor largely responsible for the directional preference in the dominant R<sup>-</sup>B<sup>0</sup> protonation state. This finding supports the electrostatic picture of the F<sub>0</sub> unidirectionality resulting from the semiquantitative and coarse-grained models.<sup>13,25,26,30</sup> Indeed, the intraprotein interactions involving R<sup>-</sup> and R176 are 4.25 and 3 times, respectively, more effective in promoting the synthesis direction than those involving the third most contributing residue, i.e., also highly conserved R169, whose interaction with R<sup>-</sup> seems to favor the synthesis too.

Since strengthening of the electrostatic attraction between pairs of oppositely charged residues over the course of the rotation is accompanied by their dehydration, the interactions of R<sup>-</sup>, R176, and R169 with water partially counteract the

intraprotein preference by favoring the hydrolysis direction (see Figure S12). In all cases, interactions with lipid molecules have mostly negligible effect on directionality.

To directly test the pivotal role of the central arginine (here R176) in differentiating the rotation energetics in the synthesis vs hydrolysis direction, we further determined how its mutation to alanine (R176A) affects the free energy landscape governing the rotary motion of the c-ring around 0° (Figure 4A). As seen from the comparison with the wild type profiles, the R176A mutation leads to a striking reduction of the barrier to rotation in the hydrolysis direction (by ~15 kcal/mol) while having only a limited effect on the free energy in the synthesis direction. Thus, upon removal of the central arginine, the energy landscape becomes roughly symmetric around 0° implying almost no kinetic preference for either of the directions (in fact, hydrolysis seems to be slightly favored). Similar rotation rates in both directions indicate that the R176A mutant should show a severe slippage between the proton flux and the mechanical output (and consequently ATP synthesis), as a substantial fraction of protons would be transported to the R site and released after only 36° rotation in the hydrolysis direction. This finding provides a possible mechanistic explanation for the rotation-uncoupled proton transport observed previously upon this mutation<sup>24,35</sup> and could be directly tested in single-molecule imaging experiments. Importantly, the removal of the second strongest interaction partner of the R<sup>-</sup>, R169, retains the asymmetry of the profile around 0° and thereby the wild-type kinetic preference for synthesis, only reducing the height of the barriers in both directions (Figure S16).

Comparison of the residue–residue interactions between the wild type and R176A mutant (see Figure S10) further substantiates the critical role of electrostatic attraction between the central arginine and the deprotonated R-site carboxylate in promoting the unidirectional rotation in the synthesis direction. This simple mechanism implies that any pair of oppositely charged residues could work in a similar manner.



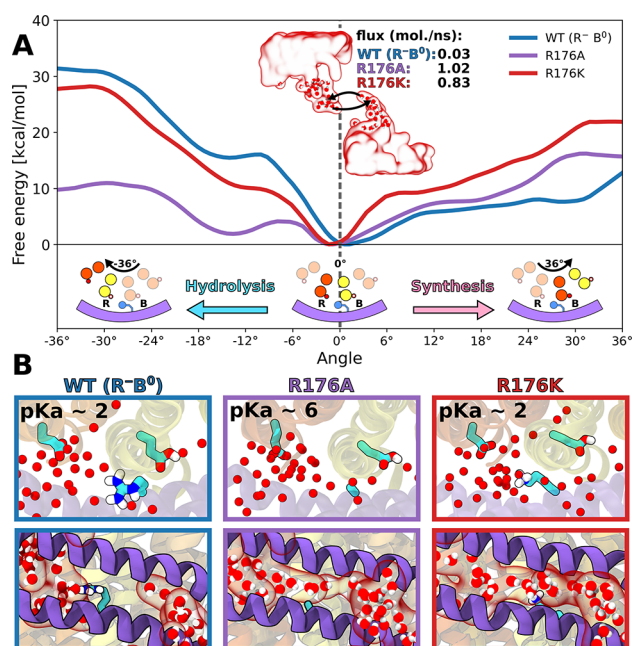


**Figure 4.** (A) Response of the free energy profile for the  $F_0$  rotation to the mutations of the central arginine (R176). Inset shows the calculated water flux between the two half-channels. (B) (Top) Calculated  $pK_a$ 's of the R-site carboxylate and (bottom) representative distribution of water molecules around the position 176 for the WT protein and the two arginine substitutions. For convergence of the free energy profiles, see Figure S4 and Figures S14 and S15.

Indeed, the c-ring glutamate (here E59) can occasionally be replaced by aspartate without abolishing the directionality, e.g., in some Gram-negative bacteria, including *E. coli*. In contrast, arginine cannot be replaced by any other residue, including lysine, i.e., the only other residue positively charged at physiological conditions. To explore why this substitution might be detrimental, we first determined and compared the hydrolysis and synthesis free energy profiles for the lysine mutation (R176K) that was also previously shown to inhibit the ATP-driven proton pumping activity.<sup>24</sup> It is clear from Figure 4A that the synthesis profile is markedly steeper for R176K than for the wild type protein such that the barrier to rotation in the synthesis direction is much more pronounced; e.g., for the  $0$ – $6^\circ$  range the barrier is  $\sim 7.5$  kcal/mol higher which renders the rotation rate 5 orders of magnitude slower compared to WT. Since electrostatic attraction between K176 and the R-site carboxylate (see Figure S11) preserves a relatively high ( $\sim 12$  kcal/mol) barrier to the rotation in the hydrolysis direction (Figure 4A), we predict that in the R176K mutant the c-ring cannot rotate away from  $0^\circ$  in either of the directions on physiologically relevant time scales. This finding explains the previous reports that the R176K mutant is unable to couple the proton motive force to ATP synthesis but, at the same time, it does not exhibit futile proton leakage as that caused by the R176A mutation.<sup>24</sup>

Because the side chain of K176 is much more flexible than that of R176 (root-mean-square fluctuation of  $0.072$  vs  $0.021$  nm<sup>2</sup>, respectively), it could be expected to interact with the carboxylate in the release site less favorably and thus lead to an undesired increase of its  $pK_a$ . To test this, we computed  $pK_a$  of the R-site carboxylate in the R176K mutant and, as a control, in the R176A mutant (Figure 4B). We found that both positively charged residues, arginine and lysine, stabilize the

deprotonated state of the carboxylate to a similar extent, lowering its  $pK_a$  by  $\sim 5$  units from a value of  $6.9 \pm 0.1$  calculated for the R176A mutant to  $1.9 \pm 0.2$  (WT) and  $2.2 \pm 0.4$  (R176K). Since the effect on  $pK_a$  of the R-site carboxylate does not depend on the exact nature of a positively charged residue, we conclude that it alone cannot explain strict conservation of the central arginine.

Having found no significant differences in the interactions with the R-site carboxylate, we turned to examining whether arginine and lysine, given their position in between the B and R sites, may cause different behavior of water molecules in the two half-channels. To this end, we determined average water densities in the  $F_0$  half-channels for the wild type protein as well as for both mutants: R176K and R176A. As can be seen in Figure 4B and Figure S1, the arginine side chain at position 176 acts as a “plug” that separates water density into two well-defined half-channels. In contrast, in both mutants the half-channels are not disconnected anymore but form a continuous aqueous pore through which water molecules can rapidly diffuse across the membrane. Specifically, we calculated the water flux between the two half-channels to be 2 orders of magnitude larger in both mutants than in the wild type ( $0.83$ ,  $1.02$ , and  $0.03$  molecules/ns, for R176K and R176A and WT, respectively). An unexpectedly high increase in the flux observed for R176K seems to arise from a fact that much more conformationally flexible lysine cannot act as an efficient water plug (see Figure S17). One could expect that the connected channel can also allow protons to leak across the membrane via Grotthuss mechanism downhill the gradient in a manner uncoupled from the c-ring rotation. Such rotation-uncoupled proton leakage has indeed been observed for the alanine mutant by Mitome et al.,<sup>24</sup> who showed that even when the c-ring is fused with the  $\alpha$ -subunit and thus unable to rotate, the  $F_0$  can still act as a proton channel when the central arginine is substituted by alanine. Although the continuous water channel is also predicted to be present in the R176 K mutant (Figure 4B, bottom), the lysine mutation has not been observed to lead to the uncoupled proton leakage.<sup>24</sup> We hypothesize that in this case protons are unable to move directly through the continuous channel from the binding to release site because of the electrostatic repulsion with the lysine.

To sum up, we found that the free energy landscape governing the  $F_0$  rotation is highly asymmetric around the initial position of the c-ring ( $0^\circ$ ), and thus rotation in the synthesis direction is strongly preferred, consistent with the motor's directionality and high efficiency of energy conversion. Importantly, this kinetic preference arises from the interplay between the intraprotein interactions and the energetics of protonation of carboxylates in the binding (B) and release (R) half-channels, consistent with recent coarse-grained simulations.<sup>13,30</sup> Specifically, we predicted that at  $0^\circ$  the B site is predominantly protonated and the R site deprotonated, and hence their  $pK_a$ 's seem to be fine-tuned to the direction of the proton gradient, accelerating the proton flow through  $F_0$  under physiological conditions. In agreement with simple early models and coarse-grained simulations,<sup>13,30</sup> our energetic analysis demonstrated that in this dominant protonation state the main contribution accounting for the much lower activation barrier in the synthesis direction is the attraction between the strictly conserved arginine in the  $\alpha$ -subunit (R176 in the yeast  $F_0$ ) and the deprotonated carboxylate at the R site. By recomputing the free energies for the R176A mutant, we

further confirmed this finding, showing that in the absence of R176 the directionality of  $F_o$  is largely abolished and the  $pK_a$  of the R site unfavorably increases by 5 units. Furthermore, the alanine mutation causes the B and R aqueous half-channels, which are well-separated by R176 in the wild type, to join in a single continuous pore through which water can readily move across the membrane. Along with the abolished directionality, the existence of this shortcut provides mechanistic explanation for the previously reported uncoupled proton transport caused by removal of the arginine side chain. Finally, we found that a positively charged residue, lysine, substituted for R176 facilitates deprotonation of the R site and preserves a high barrier to rotation in the hydrolysis direction similar to the arginine. However, it also markedly increases the barrier in the synthesis direction which slows down the rotation by several orders of magnitude, further explaining why arginine has to be conserved to ensure efficient coupling between proton translocation and rotary motion in the  $F_o$  motor.

## ■ ASSOCIATED CONTENT

### SI Supporting Information

The Supporting Information is available free of charge at <https://pubs.acs.org/doi/10.1021/acs.jpcllett.1c03358>.

Detailed description of computational methods; additional discussion of  $pK_a$  of functional residues; additional analyses of unbiased and free energy simulations; raw data used for interaction analysis (PDF)

## ■ AUTHOR INFORMATION

### Corresponding Author

Jacek Czub – Department of Physical Chemistry, Gdansk University of Technology, 80-233 Gdansk, Poland; BioTechMed Center, Gdansk University of Technology, 80-233 Gdansk, Poland; [orcid.org/0000-0003-3639-6935](https://orcid.org/0000-0003-3639-6935); Email: [jacek.czub@pg.edu.pl](mailto:jacek.czub@pg.edu.pl)

### Authors

Antoni Marciniak – Department of Physical Chemistry, Gdansk University of Technology, 80-233 Gdansk, Poland; [orcid.org/0000-0002-6859-869X](https://orcid.org/0000-0002-6859-869X)

Pawel Chodnicki – Department of Physical Chemistry, Gdansk University of Technology, 80-233 Gdansk, Poland

Kazi A Hossain – Department of Physical Chemistry, Gdansk University of Technology, 80-233 Gdansk, Poland

Joanna Slabonska – Department of Physical Chemistry, Gdansk University of Technology, 80-233 Gdansk, Poland

Complete contact information is available at: <https://pubs.acs.org/doi/10.1021/acs.jpcllett.1c03358>

### Notes

The authors declare no competing financial interest.

## ■ ACKNOWLEDGMENTS

We thank Dr. Miłosz Wieczór for helpful discussions and critically reading the manuscript. This work was funded by the Polish National Science Centre under Sonata Bis Grant 2017/26/E/NZ2/00472. This research was supported in part by PL-Grid Infrastructure. Computational resources were provided also by the TASK (Gdansk), WCSS (Wroclaw), and ICM (Warsaw) Centers.

## ■ REFERENCES

- (1) Mitchell, P. Coupling of phosphorylation to electron and hydrogen transfer by a chemi-osmotic type of mechanism. *Nature* **1961**, *191*, 144–148.
- (2) Abrahams, J. P.; Leslie, A. G. W.; Lutter, R.; Walker, J. E. Structure at 2.8 Å resolution of F1-ATPase from bovine heart mitochondria. *Nature* **1994**, *370*, 621–628.
- (3) Stock, D.; Leslie, A. G. W.; Walker, J. E. Molecular Architecture of the Rotary Motor in ATP Synthase. *Science* **1999**, *286*, 1700–1705.
- (4) Sambongi, Y.; Iko, Y.; Tanabe, M.; Omote, H.; Iwamoto-Kihara, A.; Ueda, I.; Yanagida, T.; Wada, Y.; Futai, M. Mechanical Rotation of the c Subunit Oligomer in ATP Synthase (F0F1): Direct Observation. *Science* **1999**, *286*, 1722–1724.
- (5) Guo, H.; Bueler, S. A.; Rubinstein, J. L. Atomic model for the dimeric FO region of mitochondrial ATP synthase. *Science* **2017**, *358*, 936–940.
- (6) Steed, P. R.; Fillingame, R. H. Subunit a Facilitates Aqueous Access to a Membrane-embedded Region of Subunit c in Escherichia coli F1F0 ATP Synthase. *J. Biol. Chem.* **2008**, *283*, 12365–12372.
- (7) Hahn, A.; Vonck, J.; Mills, D. J.; Meier, T.; Kühlbrandt, W. Structure, mechanism, and regulation of the chloroplast ATP synthase. *Science* **2018**, *360*, eaat4318.
- (8) Ishmukhametov, R.; Hornung, T.; Spetzler, D.; Frasch, W. D. Direct observation of stepped proteolipid ring rotation in E. coli FoF1-ATP synthase. *EMBO Journal* **2010**, *29*, 3911–3923.
- (9) Fillingame, R. H.; Angevine, C. M.; Dmitriev, O. Y. Coupling proton movements to c-ring rotation in F1Fo ATP synthase: Aqueous access channels and helix rotations at the a-c interface. *Biochimica et Biophysica Acta - Bioenergetics* **2002**, *1555*, 29–36.
- (10) Vik, S. B.; Antonio, B. J. A mechanism of proton translocation by F1F0 ATP synthases suggested by double mutants of the a subunit. *J. Biol. Chem.* **1994**, *269*, 30364–30369.
- (11) Rastogi, V. K.; Girvin, M. E. Structural changes linked to proton translocation by subunit c of the ATP synthase. *Nature* **1999**, *402*, 263–268.
- (12) Feniouk, B. A.; Kozlova, M. A.; Knorre, D. A.; Cherepanov, D. A.; Mulikjanian, A. Y.; Junge, W. The proton-driven rotor of ATP synthase: Ohmic conductance (10 fS), and absence of voltage gating. *Biophys. J.* **2004**, *86*, 4094–4109.
- (13) Kubo, S.; Niina, T.; Takada, S. Molecular dynamics simulation of proton-transfer coupled rotations in ATP synthase FO motor. *Sci. Rep.* **2020**, *10*, 8225.
- (14) Watanabe, R.; Tabata, K. V.; Iino, R.; Ueno, H.; Iwamoto, M.; Oiki, S.; Noji, H. Biased Brownian stepping rotation of FoF1-ATP synthase driven by proton motive force. *Nat. Commun.* **2013**, *4*, 1631.
- (15) Yanagisawa, S.; Frasch, W. D. Protonation-dependent stepped rotation of the F-type ATP synthase c-ring observed by single-molecule measurements. *J. Biol. Chem.* **2017**, *292*, 17093–17100.
- (16) Dimroth, P.; von Ballmoos, C.; Meier, T. Catalytic and mechanical cycles in F-ATP synthases: Fourth in the Cycles Review Series. *EMBO Rep.* **2006**, *7*, 276–282.
- (17) Junge, W.; Lill, H.; Engelbrecht, S. ATP synthase: an electrochemical transducer with rotatory mechanics. *Trends Biochem. Sci.* **1997**, *22*, 420–423.
- (18) Klusch, N.; Murphy, B. J.; Mills, D. J.; Yildiz, Ö.; Kühlbrandt, W. Structural basis of proton translocation and force generation in mitochondrial ATP synthase. *eLife* **2017**, *6*, e33274.
- (19) Watt, I. N.; Montgomery, M. G.; Runswick, M. J.; Leslie, A. G. W.; Walker, J. E. Bioenergetic cost of making an adenosine triphosphate molecule in animal mitochondria. *Proc. Natl. Acad. Sci. U. S. A.* **2010**, *107*, 16823–16827.
- (20) Soga, N.; Kimura, K.; Kinoshita, K.; Yoshida, M.; Suzuki, T. Perfect chemomechanical coupling of FoF1-ATP synthase. *Proc. Natl. Acad. Sci. U. S. A.* **2017**, *114*, 4960–4965.
- (21) Xing, J.; Wang, H.; von Ballmoos, C.; Dimroth, P.; Oster, G. Torque Generation by the Fo motor of the Sodium ATPase. *Biophys. J.* **2004**, *87*, 2148–2163.

(22) Aksimentiev, A.; Balabin, I. A.; Fillingame, R. H.; Schulten, K. Insights into the Molecular Mechanism of Rotation in the F<sub>o</sub> Sector of ATP Synthase. *Biophys. J.* **2004**, *86*, 1332–1344.

(23) Wehrle, F.; Kaim, G.; Dimroth, P. Molecular Mechanism of the ATP Synthase's F<sub>o</sub> Motor Probed by Mutational Analyses of Subunit a. *J. Mol. Biol.* **2002**, *322*, 369–381.

(24) Mitome, N.; Ono, S.; Sato, H.; Suzuki, T.; Sone, N.; Yoshida, M. Essential arginine residue of the F<sub>o</sub>-a subunit in F<sub>o</sub>F<sub>1</sub>-ATP synthase has a role to prevent the proton shortcut without c-ring rotation in the F<sub>o</sub> proton channel. *Biochem. J.* **2010**, *430*, 171–177.

(25) Dimroth, P.; Wang, H.; Grabe, M.; Oster, G. Energy transduction in the sodium F-ATPase of *Propionigenium modestum*. *Proc. Natl. Acad. Sci. U.S.A.* **1999**, *96*, 4924–4929.

(26) Elston, T.; Wang, H.; Oster, G. Energy transduction in ATP synthase. *Nature* **1998**, *391*, 510–513.

(27) Dimroth, P.; Wang, H.; Grabe, M.; Oster, G. Energy transduction in the sodium F-ATPase of *Propionigenium modestum*. *Proc. Natl. Acad. Sci. U. S. A.* **1999**, *96*, 4924–4929.

(28) Pogoryelov, D.; Krah, A.; Langer, J. D.; Yildiz, Ö.; Faraldo-Gómez, J. D.; Meier, T. Microscopic rotary mechanism of ion translocation in the F<sub>o</sub> complex of ATP synthases. *Nat. Chem. Biol.* **2010**, *6*, 891–899.

(29) Mukherjee, S.; Warshel, A. Realistic simulations of the coupling between the protomotive force and the mechanical rotation of the F<sub>o</sub>-ATPase. *Proc. Natl. Acad. Sci. U.S.A.* **2012**, *109*, 14876–14881.

(30) Bai, C.; Warshel, A. Revisiting the protomotive vectorial motion of F<sub>o</sub>-ATPase. *Proc. Natl. Acad. Sci. U. S. A.* **2019**, *116*, 19484–19489.

(31) Spikes, T. E.; Montgomery, M. G.; Walker, J. E. Structure of the dimeric ATP synthase from bovine mitochondria. *Proc. Natl. Acad. Sci. U. S. A.* **2020**, *117*, 23519–23526.

(32) Roh, S. H.; Shekhar, M.; Pintilie, G.; Chipot, C.; Wilkens, S.; Singharoy, A.; Chiu, W. Cryo-EM and MD infer water-mediated proton transport and autoinhibition mechanisms of V<sub>o</sub> complex. *Sci. Adv.* **2020**, *6*, No. eabb9605.

(33) Yanagisawa, S.; Frasch, W. D. pH-dependent 11° F<sub>1</sub>F<sub>o</sub> ATP Synthase Sub-Steps Reveal Insight into the F<sub>o</sub> Torque Generating Mechanism. *eLife* **2021**, *10*, e70016.

(34) Murphy, B. J.; Klusch, N.; Langer, J.; Mills, D. J.; Yildiz, Ö.; Kühlbrandt, W. Rotary substates of mitochondrial ATP synthase reveal the basis of flexible F<sub>1</sub>-F<sub>o</sub> coupling. *Science* **2019**, *364*, No. eaaw9128.

(35) Valiyaveetil, F. I.; Fillingame, R. H. On the Role of Arg-210 and Glu-219 of Subunit a in Proton Translocation by the *Escherichia coli* F<sub>o</sub>F<sub>1</sub>-ATP Synthase. *J. Biol. Chem.* **1997**, *272*, 32635–32641.